AIAA 79-1451R

Separate Treatment of Attached and Detached Flow Regions in General Viscous Flows

J. C. Wu* and U. Gulcat†
Georgia Institute of Technology, Atlanta, Ga.

A method for the separate computation of the attached region and the detached region in a general viscous flow is presented. The method is based upon a general kinematic relationship between the velocity and the vorticity fields. This relationship permits the needed boundary conditions for the boundary-layer region to be determined accurately and uniquely from a knowledge of the vorticity distribution. The difficulties of correctly predicting the "strong viscous-inviscid interaction" are eliminated by the present method. The method yields a highly efficient numerical procedure treating the boundary-layer equations in the attached region and the Navier-Stokes equations in the detached region.

Introduction

In a general viscous flow, there usually exist two distinct regions, one attached and the other detached, in which viscous effects are important. In the attached region, the flow is generally adequately described by the boundary-layer equations. In the detached region, which is considered in the present work to include separation bubbles, or recirculating features, and wakes, simplifications of the Navier-Stokes equations are only occasionally justifiable. It is well known that the solution of boundary-layer equations is a considerably simpler undertaking than that of the Navier-Stokes equations. Prevailing numerical methods for the general viscous flow problem, however, do not treat the attached and detached regions separately; the Navier-Stokes equations are solved in both regions. In consequence, highly efficient and accurate computer codes presently available for boundary-layer flows cannot be utilized in studying general viscous flows. Clearly, for such flows, a method which permits the separate treatment of attached and detached flow regions can lead to substantial reductions in computation requirements.

With prevailing methods, in order to treat the attached viscous region using boundary-layer equations, the mathematical description of the flow must include a specification of the velocity at the outer edge of the boundary layer or, equivalently, the pressure gradient along the boundary layer. In a general viscous flow with massive flow separation, the presence of "strong viscous-inviscid interaction" makes it unacceptable to determine the velocity of the boundary-layer edge through a potential flow calculation based upon the solid body shape even when boundary-layer displacement effects are accounted for. This fact represented an obstacle to a separate treatment of the attached and detached regions. Earlier proposals for removing this obstacle suggested repeated individual computations of the attached flow region, the detached flow region, and the inviscid part of the flow.[1-3] The velocity of the boundary-layer edge is then determined through an iterative matching procedure. Such a procedure can demand excessive amounts of computation for time-dependent flows where iterative computations for the two viscous regions as well as for the inviscid part of the flow need to be performed for each time step. The purpose of this paper is to present a new approach for the separate computation of the attached and detached regions. This approach is simple to adapt for either steady or time-dependent flow. The distinguishing feature of this approach is that it requires no involvement of the inviscid part of the flow. Indeed, according to the analyses presented in this paper, the usage of the expression "viscous-inviscid interaction" is unnecessary, and in fact misleading, since only the two viscous regions, not the inviscid and viscous parts of the flow, are interacting with one another. For time-dependent flows, the approach allows the separate computation of the attached and detached viscous regions without using an iterative matching procedure.

The present approach is developed on the foundation of a general kinematic relationship between the velocity and the vorticity fields. This kinematic relationship was expressed as an integral representation for the velocity vector and discussed in several earlier papers.[4-6] Utilizing this integral representation, computational approaches called the integro-differential[5-8] and integral representation[9,10] approaches were developed during the last few years. These approaches permit the solution field to be confined to the viscous part of the flow and therefore offer substantial computation advantages. It should be emphasized, however, that although the present approach of separate treatment of the attached and detached viscous regions is also based upon the integral representation for the velocity vector, methods other than the integro-differential or the integral-representation can be utilized to compute the flow in the two regions. In the present paper, the general kinematic relation and the integral representation are briefly reviewed for incompressible general viscous flows. The application of the present approach in the separate computation of the attached and detached viscous flows is then described.

Theoretical Foundation

Kinematics and Kinetics of Incompressible Flow

The subject of fluid mechanics, like other branches of mechanics, can be partitioned into its kinetic and kinematic aspects. For a viscous flow, this partition is conveniently accomplished through the use of the concept of vorticity and dilatation fields. The kinetic aspect then deals with the change of vorticity and dilatation fields due to various physical processes such as convection and diffusion. The kinematic aspect deals with the relationship between the velocity field at any given instant of time and the vorticity and dilatation fields at the same instant.[4] For an incompressible flow, the dilatation field is everywhere zero and only the vorticity

Presented as Paper 79-1451 at the AIAA 4th Computational Fluid Dynamics Conference, Williamsburg, Va., July 23-24, 1979; submitted Aug. 17, 1979; revision received May 30, 1980.

*Professor of Aerospace Engineering. Associate Fellow AIAA.
†Research Assistant, School of Aerospace Engineering.

vector ω needs to be defined. This definition is

$$\nabla \times v = \omega \tag{1}$$

where v is the velocity vector.

Equation (1) and the continuity equation,

$$\nabla \times v = 0 \tag{2}$$

form a differential description of the kinematics of incompressible flow. If the velocity field is known in the fluid region R, then the corresponding vorticity values can be established through Eq. (1) for all points in R. If the vorticity field ω is known, then the corresponding velocity values can be established by solving Eqs. (1) and (2), provided that appropriate boundary conditions for v are prescribed at the boundary B of the region. The question as to what constitute appropriate boundary conditions for the kinematics of the problem is of great importance to the solution of flow problems and is studied in this paper.

The kinetics of the incompressible flow problem is described by the vorticity transport equation

$$\frac{\partial \omega}{\partial t} = \nabla \times (v \times \omega) + \nu \nabla^2 \omega \tag{3}$$

where ν is the kinematic viscosity of the fluid, considered to be uniform here for simplicity, and t is the time. Equation (3) is obtained by taking the curl of time-dependent Navier-Stokes equations.

The kinematics and kinetics of the flow can be thought of as two interlaced problems in a numerical solution procedure. For time-dependent flows, using known information about the flow at an initial time level, new vorticity values for a subsequent time level are established by solving the kinetic vorticity transport equation (3) numerically. With these new vorticity values, corresponding velocity values for the subsequent time level are established by numerically solving the kinematic equations [(1) and (2)]. These two steps constitute a computation loop which advances the solution from the initial time level to a subsequent time level.[7]

The kinetic computation of new vorticity values and the kinematic computation of new velocity values are obviously interlaced since the kinetic computation of the convective effects in Eq. (3) requires a knowledge about the velocity field and the kinematic computation of new velocity values requires a knowledge about the vorticity field. In addition, the kinematics and kinetics of the problem are linked through boundary conditions needed for these two aspects. The present approach utilizes this linkage to eliminate the need for establishing the velocity of the boundary-layer edge. Because of the importance of this linkage in the work reported here, various aspects of this linkage are discussed in this paper.

The above discussions are applicable to steady flow problems if the steady-state vorticity transport equation, i.e., Eq. (3) with its left-hand side set to be zero, is used in the kinetic part of the computation and the computation loop just described is used to advance the solution from an old iteration level to a new iteration level. In the remainder of the present paper, only time-dependent flows are considered. The analyses and procedures presented, however, can be easily modified and utilized for steady flow problems.

Boundary Conditions for Kinematics

The present work was brought into focus by a theorem which has existed for some time. This theorem, specialized for an incompressible flow containing no sources, states that: "The motion of a fluid which fills infinite space and is at rest at infinity is determinate when the values of the vorticity are known at all points of the space. Similarly, the motion of a fluid which occupies a limited simply connected region is determinate when the values of the vorticity are known at all points in the region and the values of the normal velocity are known at all points of the region's boundary. In the case of a multiply connected region, the values of the circulation in the several independent circuits of the region must also be known."

This theorem, presented in many well-known treatises on fluid dynamics, e.g., Ref. 12, is concerned with the kinematic relationship between the velocity and vorticity fields. According to this theorem, if the vorticity field is known at any instant of time in a simply connected region R, then the following velocity condition on the boundary B of the region R is sufficient to determine the incompressible flow velocity field in R uniquely:

$$v \cdot n = f(r_B) \qquad \text{on } B \tag{4}$$

where n is the unit normal vector on B directed away from R, r_B is a position vector on B, and f is a known function of r_B. If the region R is multiply connected, then the value of circulation in the several independent circuits of the region must also be specified. In the following discussions, references to the boundary condition [Eq. (4)] imply also a knowledge about the circulation values wherever needed, although specific mentions of this need may be omitted at times. Since Eqs. (1) and (2) form a differential description of the kinematics of the flow, the theorem suggests that the boundary condition [Eq. (4)] permits a unique solution of Eqs. (1) and (2), provided that the vorticity field ω is known.

Let there be two velocity fields v_1 and v_2, each satisfying Eqs. (1) and (2). Define a third velocity field in R which is given by

$$v_3 = v_1 - v_2$$

It is obvious that v_3 is solenoidal and irrotational. In consequence, v_3 possesses a scalar potential which satisfies a Laplace equation, and is therefore uniquely determined in R if either the normal component of v_3 together with the needed circulation values or the tangential component of v_3 are prescribed on B.[13] In particular, if the prescribed normal velocity component and the needed circulation values, or the prescribed tangential velocity component, are zero everywhere on B, then v_3 is zero everywhere in R by virtue of the principle of extremum for the Laplace equation.

If v_1 and v_2 are required to have the same normal velocity component on B, then the normal component of v_3 is zero on B. For a simply connected region, v_3 is then zero everywhere in R. Thus, $v_1 = v_2$. In other words, for a simply connected region, the boundary condition [Eq. (4)] permits a unique solution of Eqs. (1) and (2). Similarly, for a multiply connected region R, if v_1 and v_2 are required to have the same circulation values in the independent circuits in addition to having the same normal velocity component on B, then v_3 is zero everywhere in R. Therefore Eq. (4) also permits a unique solution of Eqs. (1) and (2) for a multiply connected region. The analysis above proves the theorem stated earlier. It is noted further that, if v_1 and v_2 are required to have the same tangential velocity component on B, then the tangential velocity for v_3 is zero on B. Therefore v_3 is zero everywhere in R, and v_1 and v_2 are identical. In consequence, the boundary condition given below is also sufficient for the unique determination of v in R:

$$v \times n = g(r_B) \qquad \text{on } B \tag{5}$$

where g is a known function of r_B.

The above conclusions are shown in Ref. 6 to be correct for a flow past a single nonrotating solid. The present proof is more general and is valid for one or more solids undergoing translation and/or rotation.

Consider a viscous flow past the exterior of one or more finite solid bodies. The fluid region is bounded internally by the solid surface(s) S and externally by a surface S_∞ infinitely far from S. If the freestream velocity and the motion of the

solid(s) are prescribed, then, with the no-slip condition on S, both boundary conditions (4) and (5) are known on S and S_∞. Although either of conditions (4) or (5) is sufficient for the unique determination of v in R, the use of both conditions (4) and (5) in a numerical procedure is legitimate provided that the two conditions are compatible with each other.[7] The word compatible is used here to explain the following circumstance. Suppose Eq. (4) is prescribed on B together with a known vorticity distribution in R. Velocity field in R, including a tangential component of v on B, is then uniquely determined. If, in addition, Eq. (5) is also prescribed on B, then this prescription must agree exactly with the tangential component of v on B uniquely determined from Eq. (4). Otherwise, Eqs. (4) and (5) are not compatible and the kinematics aspect of the flow problem is "overspecified." It is recognized that in a strict sense the prescription of both Eqs. (4) and (5), even when compatible, overspecifies the kinematics of the problem. In a numerical procedure, however, the prescription of both Eqs. (4) and (5) leads to no complication as long as the conditions are compatibly prescribed. It is noted in passing that the usual method of evaluating v is first to take the curl of Eq. (1) and, by using Eq. (2), obtain a vector Poisson's equation for v in the form

$$\nabla^2 v = -\nabla \times \omega \tag{6}$$

Equation (6) is a vector Poisson's equation. Its solution requires the prescription of both Eqs. (4) and (5).

Linkage to Extraneous Boundary Condition

The two terms on the right-hand side of Eq. (3) represent the transport of vorticity in the fluid region by the kinetic processes of convection and of viscous diffusion, respectively. The convective process describes the fact that, aside from viscous diffusion, the vorticity adheres to the individual fluid particle and moves along with it. Since the vorticity field is a vector field, it experiences turning and stretching associated with the strain rate of the fluid in three-dimensional flows. Nevertheless, this process neither creates nor destroys the vorticity. The process of viscous diffusion redistributes the vorticity in the fluid. This process again does not create or destroy the vorticity.[11] Consequently, vorticity is introduced into the fluid domain only at the solid/fluid interface[7] where the "no-slip" boundary condition provides a mechanism for the generation (or depletion) of vorticity. This vorticity spreads into the interior of the fluid domain by diffusion and, once there, is transported away by both convection and diffusion. If the flow Reynolds number is not low, then the vorticity spreads only a short distance from the solid surface by diffusion before being carried away with the fluid. Thus a large region ahead and to the side of the solid surface is essentially free of vorticity and is inviscid. Furthermore, since the flow is nearly parallel to the solid surface in the attached viscous region, this region is thin compared to the dimension of the solid(s) in a high Reynolds number case. The integro-differential and integral-representation methods[5-10] were developed to exploit the fact that the vortical region of the flow represents only a small part of the total flowfield – they permit the confinement of the solution field to the vortical region. The present work is aimed at utilizing boundary-layer simplifications in computing the flow in the thin attached viscous region of the flow. Two-dimensional external flows are described in this paper to demonstrate the use of the numerical procedures that have been developed. The analyses presented are also valid for three-dimensional flows, although the algebraic operations required in three-dimensional problems are considerably more tedious.

Let the plane of the flow be the x-y plane in a Cartesian coordinate system x, y, z. The x and y components of the velocity vector are designated u and v, respectively. The vorticity vector is directed in the z direction. The vector vorticity transport equation becomes, for this two-dimensional flow, a scalar equation

$$\frac{\partial \omega}{\partial t} = -\frac{\partial (u\omega)}{\partial x} - \frac{\partial (v\omega)}{\partial y} + \nu\left[\frac{\partial^2 \omega}{\partial x^2} + \frac{\partial^2 \omega}{\partial y^2}\right] \tag{7}$$

Equation (7) is valid in the fluid domain. On the solid boundary S, the local generation or depletion of vorticity is not described by the kinetic processes of vorticity transport. Therefore, "boundary values" of ω on the solid boundary may not be computed by solving Eq. (7). However, these vorticity boundary values are needed to solve Eq. (7) and to initiate and proceed with the numerical solution for the vorticity field. Since vorticity values on S are not known directly from the prescribed solid motion, the expression "extraneous boundary condition" has been used[6] to describe the vorticity boundary condition on S. As it turns out, this extraneous boundary condition is associated with the kinematic restriction on the vorticity distribution discussed at the end of the preceding section. This linkage between the extraneous boundary condition and the kinematic restriction can be described best through an integral representation for the velocity vector[4,7]:

$$v(r,t) = -\frac{1}{2\pi}\left[\int_R \frac{\omega_0 \times (r_0 - r)}{|r_0 - r|^2}\, dR_0 - \oint_B \frac{f_0 (r_0 - r) - g_0 \times (r_0 - r)}{|r_0 - r|^2}\, dB_0\right] \tag{8}$$

where r is a position vector and the subscript 0 indicates that a variable or an integration is evaluated in the r_0 space, e.g., $\omega_0 = \omega(r_0, t)$.

Equation (8) is equivalent to Eqs. (1) and (2), together with boundary conditions (4) and (5), and is for the kinematics of two-dimensional incompressible flows. Integral representations have been presented also for the kinematics of three-dimensional imcompressible flows,[7] for the kinematics of both two- and three-dimensional compressible flows,[4,5] and for the kinetics of steady[9] and time-dependent[10] flows. A unique feature of the integral representation is that it permits the velocity field to be computed explicitly, point by point, in the fluid domain. This unique ability made it possible for integro-differential and integral-representation methods to confine the solution field to the vortical region of the flow.

It is noted that the first integral in Eq. (8) represents a velocity field associated with a distribution of vorticity in R. This integral is, in fact, an expression of the Biot-Savart law for a "distributed vortex." The second integral represents the contributions of the boundary conditions [Eqs. (4) and (5)] to the velocity field in R. As shown in the preceding section of this paper, if both these two conditions are prescribed, then the kinematics of the problem requires that they be prescribed compatibly. It is obvious, however, that both conditions can be established from the known solid motion and freestream velocity and that the compatibility of the conditions thus established is insured by the physics of the problem. This compatibility cannot exist for any arbitrarily specified vorticity distribution in R. In other words, the vorticity field is subject to a kinematic restriction. Since the vorticity field in the interior of the fluid domain is determined uniquely from a solution of the kinetic equation of vorticity transport, only the vorticity values on the fluid/solid interface is subject to the kinematic restriction. In consequence, the "extraneous" vorticity boundary condition is linked to the kinematic restriction.

Solution Procedure

A computation procedure for the viscous flow problem is developed in which the kinematic restriction described in the preceding section is utilized to establish the needed vorticity boundary condition. The fluid region is divided into a large

number of small cells. Cells contiguous to the solid boundary S are designated boundary cells. Cells in the fluid domain not contiguous to S are designated interior cells. With known values of v and ω in all cells at an initial time level, a computation loop to advance the solution to a subsequent time level consists of the following major steps:

1) The vorticity transport equation is solved numerically to establish new vorticity values for all interior cells.

2) The kinematic restriction is utilized to establish new vorticity values for all boundary cells.

3) The continuity and vorticity definition equations are solved to establish new velocity values corresponding to the new vorticity values.

Of the three steps listed above, the use of the integral representation is essential only in step 2. Many alternative methods are available for steps 1 and 3. Previous efforts by the first author have emphasized the development of methods that takes advantage of integral representations for step 1 and/or step 3. In the present work, however, available finite-difference methods are used for these two steps. Major emphases of the present work are the development of new and efficient computation procedures for step 2 and the utilization of boundary-layer simplifications whenever possible in steps 1 and 3. For steps 1 and 3, the solution field is partitioned into a region where boundary-layer simplifications are introduced and a region where the full Navier-Stokes equations are treated. The line of demarcation of the boundary-layer and the Navier-Stokes regions is placed significantly upstream of the separation point to avoid a possible improper use of boundary-layer equations.

Computation of Interior Vorticity Values

Equation (7) describes a mixed initial and boundary value problem. The solution of this problem is unique[16] in R_s for $t>\tau$, provided that the initial values of ω at time $t=\tau$ in R_s and the boundary value of ω on B for $t>\tau$ are prescribed.

In a numerical procedure for a time-dependent external flow, the boundary B consists of the solid surface S and another surface S_e which bounds the solution field externally. If the solution field used is sufficiently large, then the vorticity values are zero on S_e. Therefore, with the boundary condition on S established in step 2 and the velocity field established in the solution field R_e in step 3, values of ω are obtained numerically at the subsequent time level for all interior cells by solving the vorticity transport equation.

In the boundary-layer region, diffusion of vorticity in the direction tangential to S is unimportant. Equation (7) therefore reduces to

$$\frac{\partial\omega}{\partial t}=-\frac{\partial(u\omega)}{\partial s}-\frac{\partial(v\omega)}{\partial n}+\nu\frac{\partial^2\omega}{\partial n^2} \tag{9}$$

where s,n form a boundary-layer coordinate system, with n measuring the normal distance to S and s measuring the distance along the boundary from the forward stagnation point.

Equation (9) can be obtained easily from the familiar boundary-layer equations. Its use offers several computational advantages. With Eq. (9), the computation of new interior vorticity values for each new time level can be carried out using a numerical procedure that marches the solution forward in the s direction. The solution begins at the forward stagnation point and progresses in the downstream direction until the line of demarcation is reached. Vorticity values obtained on the line of demarcation, together with those on S and S_e, are then used in the solution of Eq. (7) in the Navier-Stokes region.

As stated earlier, available finite-difference methods are utilized in the present work to compute the vorticity values at the interior cells in both the boundary-layer and the Navier-Stokes regions. The specific methods used to solve the illustrative problems, described in the next section, are not new. However, because different methods can be used in the two different regions of the flow, an inherent flexibility of the overall solution procedure is introduced. It is important to note that, in high Reynolds number flows, the attached flow region is very thin in comparison to the length scale of the detached flow region. The separate treatment of the two regions allows different grids to be used for the two regions. In consequence, difficulties arising from the accommodation of the two vastly different length scales using the same grid system is removed. A further advantage of using Eq. (9) in the boundary-layer region is that, since the coordinate system s,n is body-fitted, no additional efforts are required to develop a body-fitted coordinate system for the boundary-layer region. The omission of the term representing the diffusion of vorticity in the tangential direction is consistent with the physics of the problem. In a method that does not treat the boundary-layer and the Navier-Stokes regions separately, this diffusion term is retained for the boundary-layer region. The retention of this negligible term in a numerical procedure clearly places an unnecessary demand on the procedure and may have led to spurious vorticity and other numerically generated noises observed by many investigators. In the present study, no spurious vorticity or noises is observed.

Computation of Boundary Vorticity Values

In this part of the computation, the integral representation for the velocity vector is used. For the present problem, the first integral of Eq. (8) is divided into two integrals, one over the interior cells and the other over the boundary cells. Having computed new vorticity values in step 1, the integral over the interior cell can be evaluated for each specific point r by numerical quadrature. With f and g known, the second integral of Eq. (8) can also be evaluated. Applying Eq. (8) to points r_s located on the solid boundary S, one obtains

$$\int_{R_b}\frac{\omega_0\times(r_0-r_s)}{r_0-r_s{}^2}\,dR_0=F(r_s)-2\pi v(r_s) \tag{10}$$

with

$$F(r_s)=\oint_B\frac{f_0(r_0-r_s)-g_0\times(r_0-r_s)}{|r_0-r_s|^2}\,dB_0-\int_{R_i}\frac{\omega_0\times(r_0-r_s)}{|r_0-r_s|^2}\,dR_0 \tag{11}$$

where R_b and R_i denote the regions containing the boundary cells and the interior cells, respectively, and $v(r_s)$ is known from the prescribed velocity boundary values.

Since the right-hand side of Eq. (10) is now known, the vorticity values in the boundary cells are the only unknowns to be determined. If the height of the boundary cells in the direction normal to S is very small, then Eq. (10) can be accurately approximated by

$$\oint_{S^+}\frac{\gamma_0\times(r_0-r_s)}{|r_0-r_s|^2}\,dS_0=F(r_s)-2\pi v(r_s) \tag{12}$$

where S^+ is a surface immediately adjacent to S and enclosing S, and

$$\gamma_0=\int_0^h\omega_0\,dn_0 \tag{13}$$

γ_0 is the strength of a vortex sheet representing the vorticity in the thin boundary cells. The normal and tangential components of Eq. (12) are Fredholm integral equations containing γ as the unknown function. The theory of solution of Fredholm equations is discussed extensively in several treatises, e.g., Refs. 14 and 15. It can be shown that the two-component equations of Eq. (12) are equivalent to one another. The conditions for the existence of a solution for γ

are met both for the interior flow and the exterior flow.[6] The solution for the exterior flow is not unique, but is rendered unique by the principle of conservation of total vorticity.[6] This principle states that the integration of the vorticity value over the combined fluid and solid regions is zero. That is,

$$\int_{R_\infty} \omega \mathrm{d}R = 0 \tag{14}$$

A rigorous proof of Eq. (14) for both two- and three-dimensional flows is presented in Ref. 11. Additional discussions regarding Eq. (10) are presented in Ref. 6. Values of γ for the boundary cells are obtained by numerically solving Eqs. (12) and (13). Vorticity values for the boundary cells are then obtained from Eq. (13) by approximating ω values within each cell by constants or by linear functions of n. Such approximations are accurate provided that the heights of the boundary cells are sufficiently small.

Computation of Velocity Values

The vorticity definition equation (1) may be written for the boundary-layer region of the present two-dimensional problem as

$$\omega = \frac{\partial V_n}{\partial s} - \frac{\partial V_s}{\partial n} \tag{15}$$

where V_s and V_n are the velocity components in the s and n directions, respectively. Within the boundary layer, the term $\partial V_n/\partial s$ is negligibly small in comparison to the term $\partial V_s/\partial n$. Therefore, an integration of Eq. (15) gives

$$V_s(s,n) = -\int_0^n \omega(s,n)\,\mathrm{d}n \tag{16}$$

Equation (16) allows values of the tangential velocity component in the boundary layer to be computed by a very simple numerical quadrature procedure at each s = constant station. Using the values of V_s computed, values of V_n are computed by numerically solving the continuity equation

$$\frac{\partial V_s}{\partial s} + \frac{\partial V_n}{\partial n} = 0 \tag{17}$$

The procedure for establishing values of V_n is described in detail in Ref. 17.

Values of v established from the boundary-layer solution on the line of demarcation, together with known values of v on the boundary surfaces S and S_e, permit velocity values in the Navier-Stokes region to be established.

Results and Discussions

Two test problems involving relatively simple flow geometries have been studied using the present approach. The first problem studied is that of a flow past a finite flat plate at zero angle of attack, with laminar boundary layers surrounding the plate and a vortex street in the laminar wake downstream of the plate. The second problem is that of a flow past a circular cylinder, with boundary layers on the forward part of the cylinder and a pair of counter-rotating vortices and a laminar wake downstream. In each problem, the solid body is set impulsively into motion and thereafter kept moving at a constant velocity. The primary purpose of solving these problems is to verify the usefulness of the present approach in separately treating the attached and detached flow regions. Numerical procedures employed are kept simple and unsophisticated by intention.

For the flat-plate problem studied, the flow Reynolds number based on the plate length and the freestream velocity is 14,000. The plate is considered to coincide with the $y=0$ plane. An implicit method using backward differencing in time and in the s direction and central differencing in the n direction is employed for the solution of the vorticity transport equation in the boundary-layer region. The DuFort-Frankel method is employed for the solution of the vorticity transport equation in the Navier-Stokes region. A successive over-relaxation technique is used to solve the Poisson's equation for the velocity vector in the Navier-Stokes region.

The velocity profiles in the boundary-layer region is found to have approached a steady state at a dimensionless time level of 1.4 after the impulsively started motion of the plate. The reference time used in nondimensionalization is the plate length L divided by the freestream velocity U. These profiles are found to agree very well with the well-known Blasius velocity profiles for the flat-plate problem. A sinusoidal disturbance of the stream function of the form

$$\psi = 0.98\times 10^{-4}\exp(-50.8y)\sin(12.7\times - 5.08t)$$

is introduced, with corresponding disturbances of u, v, and ω to the computed values, between the time levels 1.4 and 1.7. This disturbance triggers the roll-up of the laminar wake into discrete vortices. The roll-up phenomenon, once initiated, sustains itself without the introduction of any additional disturbances. Figure 1 shows computed filament lines compared with a photographed flow pattern behind a flat plate obtained by Taneda[18] for a Reynolds number of 15,800. Both the computed and the photographed flow patterns show the development of oscillation of the laminar wake and the subsequent appearance of discrete vortices further downstream. The senses of the vortices alternate and the wake widens downstream. The spacing between vortices of the same sense, i.e., the wave length of the wake oscillation, is about 0.3 the plate length in the upstream location where discrete vortices first appear in the wake. The computed wave length increases slightly in the downstream direction as the vortices grow larger. This fact has been observed experimentally.[18] The computed wave length lies in the lower range of the reported measurements. The computed wave length is substantially different from the wave length of the disturbance triggering the roll-up phenomenon. (The disturbance wave

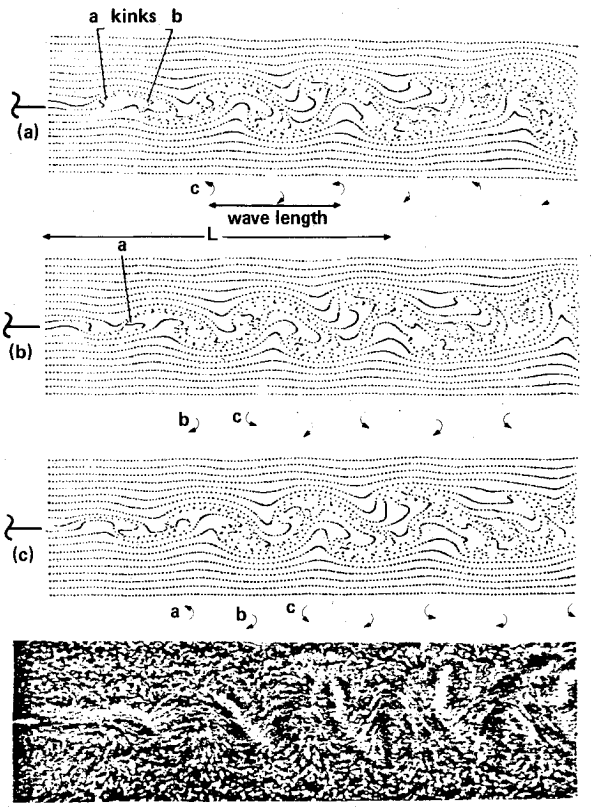

(d) Photograph (Reference 18) for LU/ν = 15,800

Fig. 1 Wake roll-up of vortices.

length is about 0.5.) This fact shows that there exists a Strouhal number for the problem which is independent of the frequency of the disturbance.

The computed filament lines shown in Fig. 1 are for three different time levels. In Fig. 1a are filament lines at a dimensionless time level of 5.3. At this time level, two kinks are observed in the filament line pattern at 0.2 and 0.35 plate lengths downstream of the trailing edge of the plate. The vortex nearest the plate is located at 0.4 plate length downstream of the trailing edge and is counterclockwise. The kinks move downstream at a speed approximately equal to the freestream speed, distorting and eventually rolling up into a clockwise vortex as shown in Fig. 1b. Figure 1b is for the time level of 5.45. This figure is in essence an inverted picture of Fig. 1a. The kinks and the leading vortex are again apparent and are located at about the same distance from the trailing edge as those in Fig. 1a. The kinks, however, are inverted from those appearing in Fig. 1a and the vortex nearest the plate is clockwise. Figure 1c show filament line at the time level 5.6. This figure is similar to Fig. 1a and shows a counterclockwise vortex nearest the plate. From these figures, it is seen that the period for the roll-up of a pair of vortices is 0.3.

For the circular cylinder problem, two cases involving flow Reynolds number of 1000 and 40,000, respectively, were studied. The differential equations are expressed in terms of polar coordinates (r,θ) attached to the cylinder and centered at the center of the cylinder. θ is the angle measured counterclockwise from the freestream direction. Vorticity values for the interior of the boundary-layer region are computed using a finite-difference method similar to that described earlier for the flat-plate problem. Vorticity values for the interior of the Navier-Stokes region are obtained by using a successive under-relaxation method for the case of Reynolds number 1000 and an alternating-direction implicit method together with upwind differencing[19] for the case of Reynolds number 40,000. Velocity values in the boundary-layer region for both cases are computed using a procedure similar to that described earlier for the flat-plate problem. For the Reynolds number 1000 case, values of the θ component of the velocity vector are computed in the detached flow region by solving a Poisson's equation using a successive-over-relaxation method. Values of the r component of the velocity vector are then computed by solving the continuity equation. For the Reynolds number 40,000 case, a Poisson's equation for the stream function is solved to obtain the stream function in the detached region of the flow. The radial and azimuthal velocity components are then computed by differencing the stream function values. The solution of the Poisson's equation is accomplished using a successive-over-relaxation method. The grid spacing in the θ direction is $\Delta\theta=\pi/20$. An exponentially expanding mesh size in the radial direction is used. For the Reynolds number 1000 case, the expansion is adjusted such a way that near the surface its size is 2% of the circular cylinder radius R and 10 radii away from the surface it increases up to 20% of R. In the case of Reynolds number of 40,000 a different expansion is arranged so that, in the radial direction, the size of the mesh is 0.2% of R on the surface and approximately $2R$ about 12 radii away from the surface.

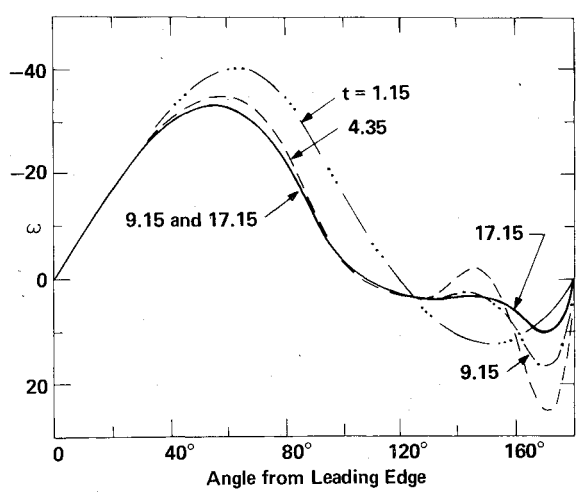

Fig. 2 Surface vorticity distribution on circular cylinder at various time levels, Reynolds number 40,000.

The evaluation of vorticity values on the surface of the cylinder is carried out using a Fourier series approximation. The θ component of Eq. (12) is used. The expression for the θ component of F is simplified in Eq. (11), by the fact that f_θ and g_θ vanish on the solid surface and line integration of the far-field boundary condition gives the term $U\sin\theta$. The result, expressed in polar coordinates, is

$$\int_0^{2\pi}\frac{\gamma_0[r_0\cos(\theta_0-\theta)-Rr_0]\,d\theta_0}{r_0^2+R^2-2r_0R\cos(\theta_0-\theta)}=-2\pi U\sin\theta$$

$$-\int_{r_0=R_1}^{R_M} r_0\,dr_0\int_{\theta_0=0}^{2\pi}\frac{\omega_0[r_0\cos(\theta_0-\theta)-R]\,d\theta_0}{r_0^2+R^2-2r_0R\cos(\theta_0-\theta)} \tag{18}$$

where U is the freestream speed, R is the radius of the cylinder, r_0 is greater than R, R_1 is the outer radius of the boundary cells, and R_M is the outer radius of the vortical region.

Let r_0 approach R. The left-hand side of Eq. (18) becomes

$$-\frac{1}{2}\int_0^{2\pi}\gamma_0\,d\theta_0+\gamma\pi \tag{19}$$

The principle of conservation of total vorticity [Eq. (14)] gives

$$-\frac{1}{2}\int_0^{2\pi}\gamma_0R\,d\theta_0=\frac{1}{2}\int_{r_0=R_1}^{R_M} r_0\,dr_0\int_{\theta_0=0}^{2\pi}\omega_0\,d\theta_0 \tag{20}$$

Placing Eqs. (19) and (20) into Eq. (18), one obtains:

$$\gamma=-2U\sin\theta\frac{1}{2\pi R}\int_{r=R_1}^{R_M} r_0(r_0^2-R^2)\,dr_0$$

$$\times\int_0^{2\pi}\frac{\omega_0\,d\theta_0}{r_0^2+R^2=-2rR\cos(\theta_0-\theta)} \tag{21}$$

The vortical region outside the boundary cells is divided into concentric rings with the jth ring in the region $R_j\le r\le R_{j+1}$. ω_0 values in the jth ring are approximated by a finite Fourier series

$$\omega_{0j}=\frac{A_0}{2}+\sum_{k=1}^{N-1}(A_{k,j}\cos k\theta_0+B_{k,j}\sin k\theta_0)+\frac{A_{N,j}}{2}\cos N\theta_0 \tag{22}$$

Placing Eq. (22) into Eq. (21) and performing the integration with respect to θ_0, one obtains the following approximate expression:

$$\gamma=-2U\sin\theta$$

$$-\left[\sum_{j=1}^{M-1}\frac{A_{0j}}{2}+\sum_{k=1}^{N-1}\left(\frac{R}{r_0}\right)^k(A_{k,j}\cos k\theta+B_{k,j}\sin k\theta)\right] \tag{23}$$

With Eq. (23), values of the strength of the vortex sheet representing the vorticity in the boundary cells are readily obtained once the coefficients of the finite Fourier series representing the vorticity in the concentric rings are established. The vorticity value at the center of each boundary

cell is then obtained by dividing the value of γ by the height of the cell.

In Fig. 2 is shown the time history of the vorticity distribution on the upper half of cylinder surface for the Reynolds number 1000. Two separation bubbles appear at the dimensionless time level of 0.2 after the initiation of the cylinder motion. The reference time used for non-dimensionalization is the cylinder radius R divided by the freestream velocity U. The separation point, determined from the sign reversal of the surface vorticity, is initially located near the trailing edge of the cylinder. This separation point moves upstream rapidly as the separation bubble grows. A pair of counter-rotating vortices become established behind the cylinder. The separation point eventually reaches a steady-state value of 108 deg from the forward stagnation point. This value is in excellent agreement with computed and experimental values reported in Ref. 20. For intermediate time levels, a very small secondary separation bubble appears inside each primary bubble. The presence of this bubble is indicated, for example, by the region of negative surface vorticity for the time level 2.18 that appears near the point 36 deg from the trailing edge. The sense of rotation of the secondary bubble is opposite to that of the primary bubble surrounding it. This secondary bubble first grows in size and then shrinks and eventually disappears. A pronounced peak in surface vorticity magnitude is observed aft of the secondary bubble. This peak survives the disappearance of the secondary bubble. The magnitude of this peak decreases slowly with time. In the major part of the flowfield, the flow is symmetric about the diameter of the cylinder in the freestream direction. Flow near the rear stagnation point, however, developed a noticeable asymmetry for the last few time levels studied. The peak surface vorticity value near the rear stagnation point was observed to be 8.9 at the upper surface and -12.2 at the lower surface for the time level 6.58. For the time level 8.58, the peak surface vorticity value at the upper surface becomes 11.9 while that at the lower surface becomes -7.3. Thus, while the averaged magnitude of the upper and lower surface vorticity decreases slowly with time, the upper and lower peak magnitudes oscillate about the average magnitude. The flow features and history of flow development described here are similar to those reported by Thoman and Szewczyk.[20] In spite of the time-dependent behavior near the rear stagnation point, flow in other parts of the flowfield is essentially steady after a time level of about 5. For example, the calculated pressure distribution on the cylinder and the total drag remain essentially unchanged between the time levels 6.58 and 8.58. The present computation is terminated at the time level 8.58.

For the Reynolds number 40,000 case the flow separates earlier, at about dimensionless time level of 0.16, and the separation point moves further upstream on the surface as the time progresses. The calculations for this case are terminated at time level of 4.80 and the separation point is located at 89 deg from the forward stagnation point at this level. The appearance of a small secondary separation bubble is observed at the inside of each primary bubble about 54 deg from the trailing edge at the dimensionless time level of 1.0. The secondary separation bubble first grows in size and in intensity, then its size remains almost constant while its intensity reduces by time. This agrees with the numerical solution given in Ref. 20.

In Fig. 3 are shown three sets of pressure distributions for the circular cylinder problem at a Reynolds number of 40,000. The distributions are 1) numerical results obtained using the present approach in which the viscous part of the flowfield is separated into a boundary-layer region and a Navier-Stokes region; 2) finite-difference results obtained by Thoman and Szewcyzk[20] treating the entire flow, including the potential and the viscous regions, on the basis of the Navier-Stokes equations, and 3) experimental results reported in Ref. 21. The agreement between the present results and experimental results is remarkably good. The small differences between the

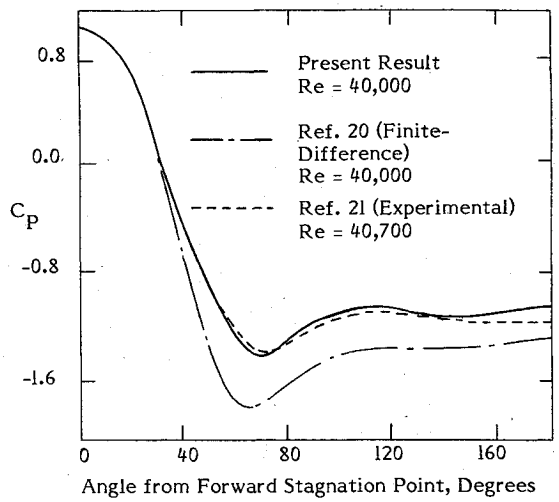

Fig. 3 Surface pressure distribution on circular cylinder.

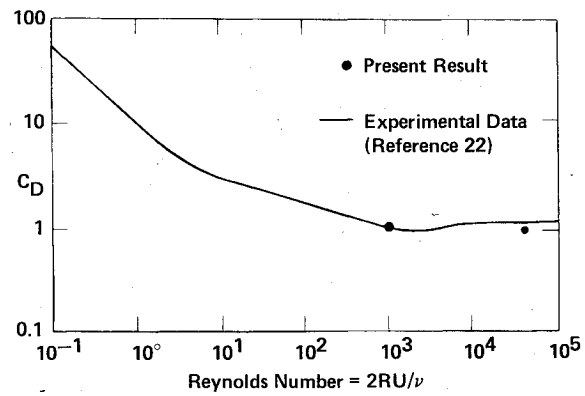

Fig. 4 Drag coefficient for circular cylinder.

present and experiment results near the rear stagnation point are expected since, in the present computation, no provision is made to model flow turbulence occurring in the recirculating flow and in the wake downstream of the cylinder. The contrast with the remarkably good agreement just described, the finite-difference results obtained treating the entire flow on the basis of the Navier-Stokes equations differ substantially from the experimental results. The pressure coefficient C_P is defined by

$$C_P = \frac{p - p_\infty}{\frac{1}{2}\rho U^2} \tag{24}$$

where ρ is the density of the fluid, p is the static pressure, and p_∞ is the freestream pressure. The pressure p is determined from the tangential pressure gradient, $\partial p/\partial s$, which is related to the normal vorticity gradient $\partial\omega/\partial n$ by

$$\frac{\partial p}{\partial s} = -\rho\nu \frac{\partial \omega}{\partial n} \qquad \text{on } S \tag{25}$$

Equation (25) is obtained from the Navier-Stokes equation by noting that the velocity vector is zero on S and

$$\omega = -\partial u/\partial n \qquad \text{on } S \tag{26}$$

Using Eq. (26), one obtains the following expression for the shear stress on the cylinder surface:

$$\tau = -\rho\nu\omega \qquad \text{on } S \tag{27}$$

Taking the components of τ and p in the freestream direction, integrating the sum of these components over the

cross section of the cylinder, and nondimensionalizing the result with respect to $\rho U^2 R$, one obtains the total drag coefficient C_D shown in Fig. 4. The computed drag coefficient for the Reynolds number 1000 case is in excellent agreement with the experimental data as presented in Ref. 22. For the case of Reynolds number 40,000, drag coefficient predicted by present method is slightly less than the experimental value.[21] This disagreement is due to low C_P values obtained in magnitude around the rear stagnation point. At this high Reynolds number it is likely that flow at the wake of the cylinder is already turbulent which increases the drag. However, for the present method wake is assumed to be laminar.

The central processer time used to advance the solution for the circular cylinder problem by one unit of dimensionless time is about 200 s on the CDC 6400 computer. As mentioned earlier, the numerical procedure used in the present work has been kept simple and unsophisticated by intention. The primary emphasis of the present work is the separate treatment of the boundary-layer and Navier-Stokes regions. No effort has been devoted in optimizing the solution procedure in each region. Previous experience with other approaches suggests that the computer time needed for the solution of the circular cylinder problem can be reduced to less than 60 s per unit nondimensional time by using more sophisticated procedures within each region of the viscous flow.

Of the 200 s required to advance the circular cylinder solution by one nondimensional unit of time, only about 10 s are needed for the boundary-layer flow, which covers about one-half of the circular cylinder surface. The computation of the flow in the Navier-Stokes region requires the major portion of the computer time since this part of computation utilizes an iterative procedure. It should be noted that, with the present approach, the boundary-layer computation requires no iteration. If the entire flow were solved using the Navier-Stokes equations, the number of iterations required would be much greater for each time step since the number of data points involved in the iterative procedure would be much greater. The circular cylinder problem at a Reynolds number of 1000 was solved again using the techniques just described, except that the Navier-Stokes equation was used for the entire flowfield. It was found that the computer time required is more than twice that required when the boundary-layer region was treated separately.

The work described in this paper represents the initial efforts in the development of the present approach to study the attached and detached flow regions separately. The results of the present study shows that this approach can be easily implemented. The method for computing the surface vorticity values developed for the circular cylinder problem can be easily adopted and used to treat problems involving more complex solid geometries through the use of a transformation technique. This surface vorticity calculation method, in fact, has already been utilized in a study of a turbulent flow past a 12% thick airfoil.[23] In addition to providing a highly efficient numerical procedure, the separate treatment of the attached and detached viscous regions removes the difficulty of simultaneously accommodating the two vastly different length scales of the two regions. In addition, it eliminates special efforts required to develop body-fitted coordinate systems for the boundary-layer region.

Acknowledgment

This research is supported by the Office of Naval Research under Contract N00014-75-C-0249.

References

[1] Crimi, P. and Reeves, B. L., "A Method for Analyzing Dynamic Stall," AIAA Paper 72-37, Jan. 1972.

[2] Seginer, A. and Rose, W. C., "A Numerical Solution of the Flow Field over a Transonic Airfoil Including Strong-Shock-Induced Flow Separation," AIAA Paper 76-330, July 1976.

[3] Murphy, J. D., "An Efficient Solution Procedure for the Incompressible Navier-Stokes Equations," *AIAA Journal,* Vol. 15, Sept. 1977, pp. 1307-1314.

[4] Wu, J. C., "Finite Element Solution of Flow Problems Using Integral Representation," *Proceedings of Second International Symposium on Finite Element Methods in Flow Problems,* International Centre for Computer Aided Design, Conference Series 2/76, June 1976, pp. 205-216.

[5] Wu, J. C., "Integral Representations of Field Variables for the Finite Element Solution of Viscous Flow Problems," *Proceedings of 1974 Conference on Finite Element Methods in Engineering,* Clarendon Press, 1974, pp. 827-840.

[6] Wu, J. C., "Numerical Boundary Conditions for Viscous Flow Problems," *AIAA Journal,* Vol. 14, August 1976, pp. 1042-1049.

[7] Wu, J. C. and Thompson, J. F., "Numerical Solutions of Time-Dependent Incompressible Navier-Stokes Equations Using an Integro-Differential Formulation," *Journal of Computers and Fluids,* Vol. 1, No. 2, 1973, pp. 197-215.

[8] Wu, J. C., Sankar, N. L., and Sugavanam, A., "A Numerical Study of Unsteady Viscous Flows Around Airfoils," *Proceedings of AGARD Symposium on Unsteady Aerodynamics,* AGARD-CP-227, Feb. 1978, pp. 24-1-18.

[9] Wu, J. C. and Wahbah, M., "Numerical Solution of Viscous Flow Equations Using Integral Representations," *Proceedings of Fifth International Conference on Numerical Methods in Fluid Dynamics, Lecture Series in Physics,* Vol. 59, Springer-Verlag, 1976, pp. 448-453.

[10] Wu, J. C. and Rizk, Y. M., "Integral-Representation Approach for Time-Dependent Viscous Flows," *Proceedings of Sixth International Conference on Numerical Methods in Fluid Dynamics, Lecture Notes in Physics,* Vol. Springer-Verlag, 1978.

[11] Wu, J. C., "A Theory for Aerodynamic Forces and Moments," Georgia Institute of Technology Report, June 1978.

[12] Lamb, H., *Hydrodynamics,* 6th Ed., Dover Publications, New York, 1945.

[13] Batchelor, G. K., *An Introduction to Fluid Dynamics,* Cambridge University Press, Cambridge, England, 1967.

[14] Gakhov, F. D., *Boundary Value Problems,* trans. by I. N. Sneddon, Pergamon Press, New York, 1966.

[15] Kellogg, O. D., *Foundations of Potential Theory,* Dover Publications, New York, 1953.

[16] Garabedian, P. R., *Partial Differential Equations,* John Wiley & Sons, New York, 1967.

[17] Wu, J. C., "On the Finite Difference Solution of Laminar Boundary Layer Problems," *Proceedings of 1961 Heat Transfer and Fluid Mechanics Institute,* Stanford University Press, Stanford, Calif., 1961, pp. 55-69.

[18] Taneda, S., "Oscillation of the Wake Behind a Flat Plate Parallel to the Flow," *Journal of the Physical Society of Japan,* Vol. 13, April 1958, pp. 418-425.

[19] Roache, P. J., *Computational Fluid Dynamics,* Hermosa Publishers, Albuquerque, N. M., 1972.

[20] Thoman, D. C. and Szewczyk, A. A., "Time Dependent Viscous Flow over a Circular Cylinder," *Physics of Fluids,* Vol. 12, Dec. 1969, pp. II-76-86.

[21] Goldstein, S., *Modern Developments in Fluid Dynamics,* Vol. II, Dover Publications, New York, 1965.

[22] Schlichting, H., *Boundary-Layer Theory,* trans. by J. Kestin, McGraw Hill Book Co., New York, 1968.

[23] Sugavanam, A., "Numerical Study of Turbulent Flow over Airfoils," Ph.D. Thesis, Georgia Institute of Technology, Atlanta, Ga., Aug. 1979.